Computer Graphics and Image Processing by Field Theory

Yoshifuru SAITO[1],
[1] Graduate School of Hosei University. Tokyo 184-8584, Japan

Field theory in physics is the most important counterpart establishing the modern physics. Starting with the Newton mechanics, any of the field problems, such as the theory of sound, light, electromagnetism reduce into solving for their field governing equations. Classical field theory had exploited the vector and variational calculus, and led to the modern quantum mechanics. Mathematically, the orthogonal functions representing the solution of field equations have led a systematical formulation of the Hilbert space theory [1].

On the other side, modern computer graphics has been started with the developments of modern high-speed digital computers. At the beginning of computer graphics, the simple primitive geometrical methodologies were widely used to construct a graphical object. The extensive spreading of the digital computers with higher performance has stimulated the expectation of the computer graphics versatilities, because the computer graphics is capable to communicate a large amount of information. In order to respond and realize, such an expectation and requirement to the computer graphics, it is not simple geometry any more, and more advanced geometry, such as the projective, topological, homotopic geometries and cellar spatial theory, must be applicable [2].

The problems of modern computer graphics to be breakthrough may be focused on the two major difficulties, one is the data quantity and the other is how to unite with the simulation technology of existent engineering as well as physics. The field theory of computer graphics described in this paper is one of the systematic approaches to remove these difficulties.

The image processing, compressing, visualizing, identifying and animating are efficiently carried out by means of the field theory. The field theory of computer graphics regards an each of the pixels as one of the potentials in vector fields. As is well known, gradient operation to the scalar potentials yields the image vector fields. A norm distribution of the field vectors generates a sketch like image. Also, an inner product between the unit directional and image vectors generates a three-dimensional shadowed image. Further spatial differential operation, i.e., divergence operation, changes the image vector into a scalar quantity called an image field source density. In electromagnetic fields, this source density corresponds to an electric charge density, while the image scalar potential corresponds to an electric scalar potential called a voltage. Such an electromagnetic fields, the voltage can be exactly evaluated by solving a partial differential (Poisson's) equation having the electric charge density as an input electric field source [3,4]. This is true in the image source density. Namely, an exact original image can be recovered from the image source density. Since the image source density can be obtained by the twice-partial differentiations, i.e., Laplacian operation, the constant and first derivative terms are essentially not included in the source density. This means that the original image is compressed in terms of the image source density while the singular point information of the original image is extracted by the Laplacian operation in homotopic sense. Even though, an efficiency of the data compression depends on each of the distinct images, data compression is always possible not loosing any original image information.

References

[1] P.M.Morse and H. Feshbach, "Methods of Theoretical Physics," McGraw-Hill, New York (1953).
[2] J.H.C.Whitehead, "Combinational Homotopy 1," Bulletin of American Mathematical Society, Vol.55, pp.213-245 1949
[3] P.P.Silvester "Modern Electromagnetic Fields", Prentice-Hall, Inc., 1968.
[4] P.P.Silvester and R.L.Ferrari, "Finite elements for electrical engineers", Cambridge University Press (1983).

Development of a New High Sensitive Eddy Current Sensor

Hiroki KIKUCHIHARA[1, a], Iliana MARINOVA[2,b] , Yoshifuru SAITO[3,c]
Manabu OHUCHI[3, d], Hideo MOGI[3,b] and Yoshiro OIKAWA[3,e]
[1] Graduate School of Hosei University, Tokyo 184-8584, Japan
[2] Technical University of Sofia, Sofia 1756, Bulgaria
[3] Denshijiki Industry Co., Ltd, Tokyo 115-0051, Japan
[a]hiroki.kikuchihara.6e@stu.hosei.ac.jp, [b]iliana@tu-sofia.bg, [c]ysaito@hosei.ac.jp
[d]et.factory@emic-jp.com, [f]oikawa@emic-jp.com

Keywords: Eddy current, Nondestructive testing

Abstract. Eddy current testing (ECT) is one of the most representative nondestructive testing methods for metallic materials, parts, structures and so on. Operating principle of ECT is based on two major properties of the magnetic field. One is that alternating magnetic field induces eddy current in conducting materials. Thereby, an input impedance of the magnetic field source, i.e., electric source, depends on the eddy current path. Second is that the magnetic field distribution depends not only on the exciting but also on the reactive magnetic fields caused by the eddy currents in targets. Former and latter are the impedance sensing and magnetic flux sensing types, respectively.

This paper concerns with an optimization of a new magnetic flux sensing type sensor named "∞ coil". Exciting and sensing coils are composed of ∞ shape coil and a finite length solenoid coil wound on ferrite bar, respectively. Development of this ∞ coil fully depends on the 2D and 3D finite elements method modeling. According to the simulation results, we have worked out two types of ∞ coils. Practical experiments reflect the validity of both simulation and design aims, quite well. Thus, we have succeeded in developing ∞ coil having a higher sensibility compared with that of conventional one.

Introduction

Modern engineering products such as air-plane, automobile, smart building, high speed train and so on are essentially composed of metallic materials for forming the shape of product, suspending the mechanical stress and constructing the structural frames. In particular, the mass transportation vehicles, e.g. large air plane, high-speed train, express highway bus and so on, carrying a large number of people are required ultimately high safety as well as reliability.

To keep the safety, nondestructive testing to the metallic materials is one of the most important technologies because most of the structure materials are composed of the metallic materials.

Various nondestructive testing methods, such as eddy current testing (ECT), electric potential method, ultrasonic imaging and x-ray tomography, are currently used. Among these methods, ECT needs not complex electronic circuits and direct contact to target. Furthermore, a target whose major frame parts are composed of conductive metallic materials can be selectively inspected by ECT [1,3].

In this paper, a new ECT sensor coil named "∞ coil" is proposed. Development of this ∞ coil fully depends on the 2D and 3D finite elements method modeling and also optimizes the eddy current testing methodology.

The most important key idea of the ∞ coil is in setting the sensor coil in the lowest magnetic field space caused by the exciting coils, because this sensor coil is capable of catch only the magnetic fields caused by the detour eddy currents flowing around a defect. This paramount important key idea has been yielded by carrying out the intensive 2D finite elements simulations. After that 3D finite elements simulation has been carried out to check up the validity of this key idea.

Thus, we have succeeded in innovating and optimizing a new high sensibility eddy current sensor "∞ coil" by means of the 2D and 3D finite elements simulations [2,3].

New ECT Sensor Coil

Operating principle of the separately installed sensing coil type is fundamentally based on that the sensing coil catches the magnetic field intensity variation caused by the detour eddy currents flowing around a defect in the target metallic materials.

To realize this, three methodologies could be considered. The first detects the variation of entire magnetic fields caused by both exciting and eddy currents. In this case, the sensing coil detects the magnetic fields distribution caused by the detour eddy currents around defects among the entire magnetic fields. The second is that the sensing coil surface is installed in a perpendicular direction to an exciting coil surface. This means that the sensing coil never induce an electric voltage caused by the exciting fields because the surface of sensing coil always parallels to the exciting magnetic fields, so that this sensing coil is capable of selectively catching the magnetic fields caused by the detour eddy currents around a defect. This type of sensor has high liftoff characteristics compared with those of the first one. The final third one is that the sensing coil is set on the zero exciting magnetic fields space in addition to the second one coil layout. This final one is capable of catching only the magnetic fields caused by the detour eddy currents around a defect, and has been innovated in this paper by a series of the intensive finite elements simulations.

At the beginning of our new sensor project, to concentrate the magnetic fields, the two exciting coils whose magneto-motive forces becomes in additive were employed, as shown in Fig.1.

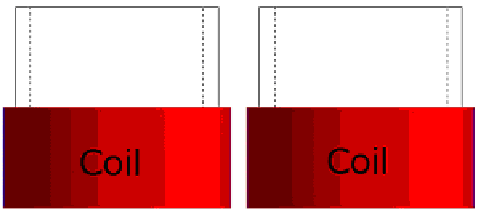

Fig. 1 Two exciting coils

To decide a location of sensing coil whose surface is orthogonal to the exciting magnetic fields, we have carried out a lot of 2D finite elements simulations. As a result, it is found that there is nearly zero exciting field space between the two exciting coils. This leads to our ∞ coil. Since the zero exciting magnetic fields condition in addition to the orthogonal coil surface layout to the exciting magnetic fields enhances the sensibility of ∞ coil in an ultimately. Fig 2(a) shows an exciting magnetic field intensity distribution. In this figure, it is possible to find the zero magnetic fields space between the two parallel exciting coils. According to this simulation result, we put on a ferrite bar at the bottom surface of the two exciting coils in order to enhance the sensibility of sensor coil. As shown in Fig.2(b), setting the ferrite bar hardly disturb the exciting magnetic fields intensity distribution. Thus, winding around the sensor coil around the ferrite core leads to an ultimately optimized high sensibility ECT sensor, i.e., ∞ coil.

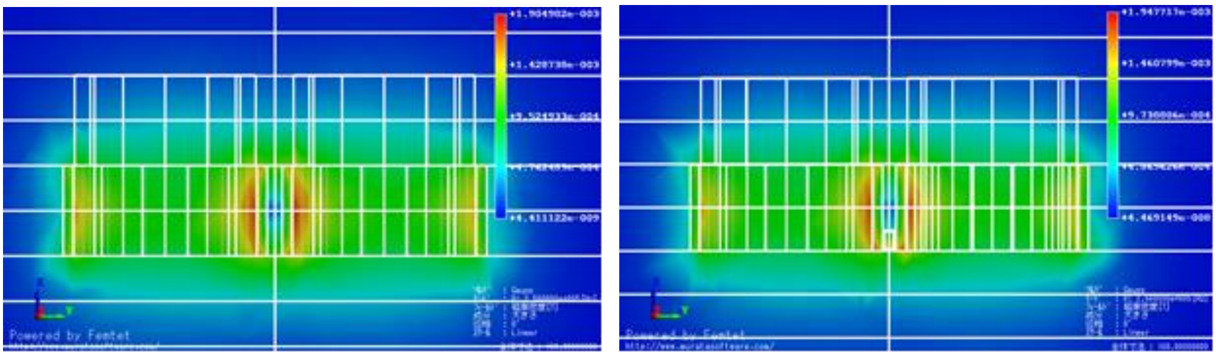

(a) Without ferrite bar (b) With ferrite bar

Fig. 2 Magnetic fields intensity

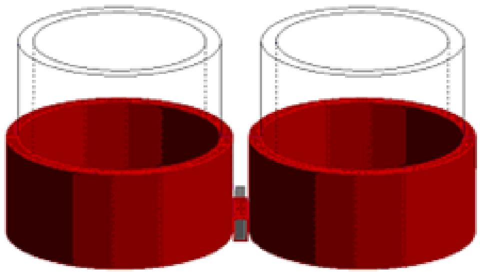

Fig. 3 3D simulation model of the ∞ coil

Table 1 Various constants used in the 3D simulation.

Exciting coil	
Coil outer diameter	22.4mm
Coil inner diameter	20mm
Coil length	10mm
Number of turn	75
Input current(peak)	250mA
Frequency	256kHz
Sensing coil	
Coil outer diameter	1.4mm×2.4mm
Coil inner diameter	1mm×2mm
Coil length	6mm
Number of turn	100
Axis core	JFEferrite_MB1H _23°C

To evaluate the validity of our ∞ coil performance, we employed a 3D simulation model shown in Fig.3.Table 1 lists various constants used in the 3D simulation. The eddy currents in a plane target located under the two exciting coil surfaces are shown in Fig. 4, where the two adjacent exciting coils side to the no-defect, 0 degree, 90 degree and 45 degree line defects are shown in Figs. 4(a),4(b),4(c) and 4(d), respectively.

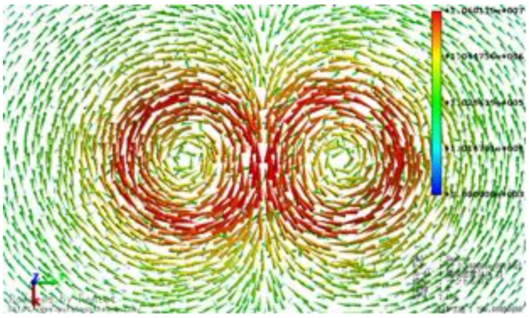

(a) No defect

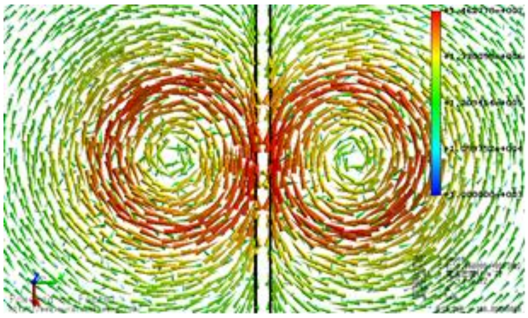

(b) 0 degree defect

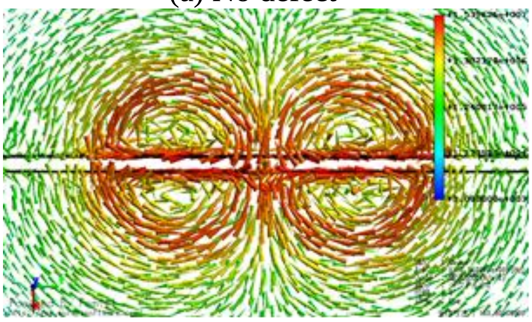

(c) 90 degree defect

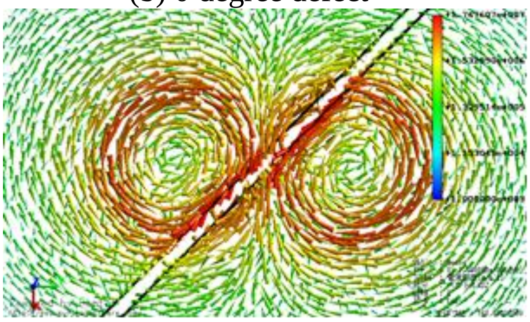

(d) 45 degree defect

Fig. 4 Eddy currents in a plane metallic target.

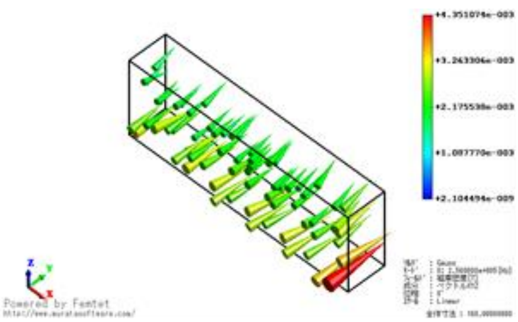

(a) No defect

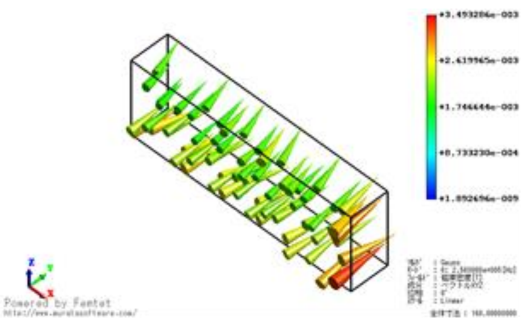

(b) 0 degree defect

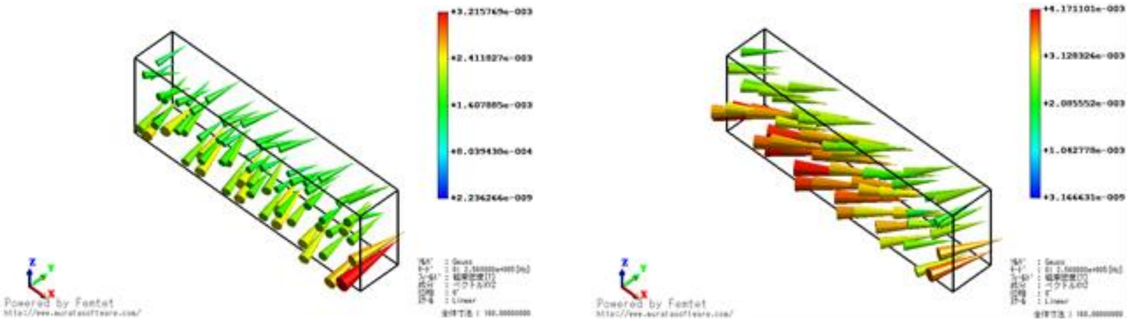

(c) 90 degree defect (d) 45 degree defect

Fig. 5 Magnetic flux density vector distributions in the ferrite bar

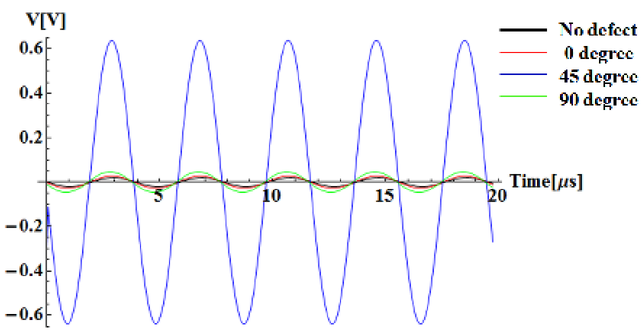

Fig. 6 Induced voltages in the sensor coil

Fig. 5 shows the magnetic flux density vector distribution corresponding to that of eddy currents in Fig. 4. Observe the magnetic flux density vector distributions in Fig. 5 reveals that the sensing coil wound around the ferrite bar could be induced the electric voltages not the cases (a), (b), (c) and (d). The induced voltages of the sensor coil under the conditions (a)-(d) in Figs. 4 and 5 are shown in Fig. 6. Observing the induced voltages in Fig.6 reveals that the case (d) yields the highest voltage.

Experiment

We employed two coppers plate having 1mm thickness as target metal plates. One has no defect and the other has a line defect having 2mm width. Also, we worked out a prototype of the ∞ coil. Table 2 lists various constants of the prototype ∞ coil. We used two exciting coils and one sensing coil having ferrite core. Fig. 7 shows a picture of the prototype ∞ coil. The physical dimensions of this prototype ∞ coil are corresponding to the 3D simulation model shown in Fig.3.

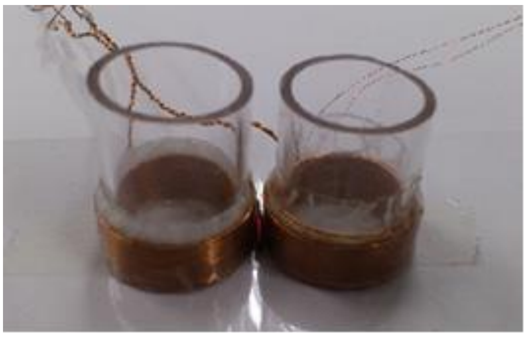

Fig.7 Picture of the prototype ∞ coil.

Table 2 Various constants of the prototype ∞ coil.

Exciting coil	Conductor length	4.7m
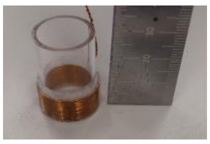	Diameter of conductor	0.4mm
	Coil outer diameter	23mm
	Coil inner diameter	20mm
	Coil length	10mm
	Number of turn	75
	Number of coil layers	3
	Number of coils	2
Sensing coil	Conductor length	60cm
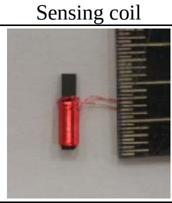	Diameter of conductor	0.1mm
	Axis core	Ferrite bar (MnZn)
	Coil outer diameter	1.4mm×2.4mm
	Coil inner diameter	1mm×2mm
	Coil length	6mm
	Number of turn	100
	Number of coil layers	2

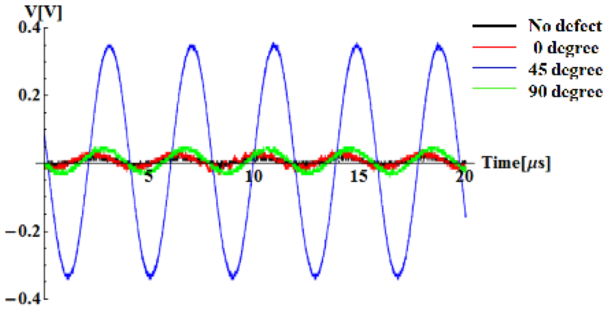

Fig.8 Measured voltages of the practical sensing coil.

Fig. 8 shows the measured voltages corresponding to that of cases in Figs. 4 and 5. Even though the peak measured voltage is somewhat smaller than those of Fig.6, sensing characteristics of the prototype ∞ coil well correspond to that of Fig. 6. Thus, we have succeeded in innovating new type eddy current sensor "∞ coil" by means of the 2D and 3D finite elements simulations.

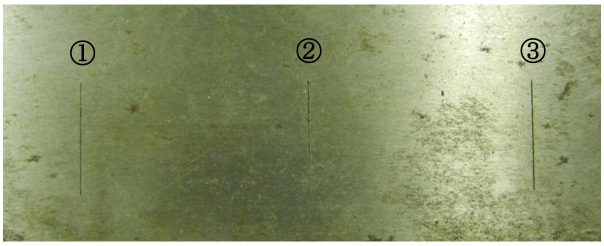

Fig. 9 Target piece with three defects.

Fig. 10 ET-5002 produced by Denshijiki Industry Co., Ltd.

To compare ∞ coil with conventional ECT sensors, we measured liftoff characteristics of three type sensors. Fig. 9 shows a target piece which is composed of SS400 steel. The target piece has three defects which are 20 mm length, 0.2 mm width and 0.2, 0.3, 0.4 mm depth on the surface. The defect was made by the electrical discharge machining. We moved the tested three ECT sensors with 50mm/s speed and measured the signal of defect by means of the commercial based signal processing device "ET-5002", shown in Fig. 10. Operating principle of the ET-5002 is that the equilibrium balanced condition of the bridge circuit picks up only the discontinuity of signals when the sensor runs over the defect. We employed 256 kHz operating frequency. Liftoff was changed every 1mm from 1mm to 10mm. The gain in dB, high pass filter in Hz, low pass filter in Hz and the liftoff distances were set up to the ET-5002.

Table 3 Specification of the tested three sensors

∞ coil			
Sensing coil		Exciting coil	
Diameter of conductor:	0.1mm	Diameter of conductor:	0.12mm
Axis core:	Ferrite bar (MnZn)	Axis core:	No
Coil inner diameter:	0.5mm×2mm	Coil inner diameter:	6mm
Coil length:	4mm	Coil length:	6mm
Number of turn:	100	Number of turn:	100
Number of coil layers	3	Number of coil layers	3
Number of coils:	1	Number of coils:	2
Magnetic flux sensing type sensor			
Sensing coil		Exciting coil	
Diameter of conductor:	0.1mm	Diameter of conductor:	0.12mm
Axis core:	Ferrite bar (MnZn)	Axis core:	No
Coil inner diameter:	1mm×2mm	Coil inner diameter:	4mm
Coil length:	10mm	Coil length:	12mm
Number of turn:	50	Number of turn:	100
Number of coil layers	2	Number of coil layers	1
Number of coils:	2	Number of coils:	1
Impedance sensing type sensor			
Sensing coil		Exciting coil	
Diameter of conductor:	0.1mm		
Axis core:	Ferrite bar (MnZn)		
Coil inner diameter:	0.5mm×2mm		
Coil length:	10mm		
Number of turn:	100		
Number of coil layers	3		
Number of coils:	2		

Table 3 lists specifications of ∞ coil, Magnetic flux sensing type sensor and Impedance sensing type sensor. The size of sensing coil and exciting coils of the ∞ coil were constructed by means of the optimization based on the 3D finite elements simulations.

Magnetic flux sensing and Self-induction type sensors are the commercial based products of Denshijiki Industry Co., Ltd.

Both of the sensors are based on the differential property of 8 shape coil. The difference between them is that the magnetic flux sensing type employs an independent exciting coil surrounds 8 shape coil. On the other side, the exciting magnetic fields of self-induction type are produced by the currents flowing through the 8 shape coil.

Thus, both two commercial based sensors are capable of detecting the defects in the target materials with high sensibility.

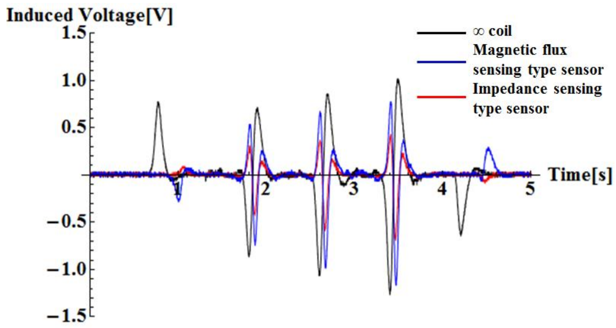

Fig. 11 Induced voltage (liftoff = 2mm)

Fig. 11 shows induced voltages of the three type sensors when passing close to and get away from a target piece having a line defect.

Observe the signal makes it possible to find the 5 distinct peaks in each of the sensor signals. Among 5 peaks, the first and last ones are occurred when the sensors are getting close and away from the target. Thereby, let us focus on the 3 peaks caused by the three defects excepting the first and last peaks.

Magnitudes of these 3 peaks depend on each of the defect depths while every sensor is used. Among the signals in Fig. 11, the signal obtained by ∞ coil is the most sensitive compared with that of the others. To evaluate a more detailed characteristic, we focus on the signal caused by defect whose depth is 0.2mm.

Fig. 12 shows the peak induced voltages when changing the liftoff distances from 1mm to 10mm. It is found that the ∞ coil is superior in most of liftoff cases. However, we confront to intensive difficulty when obtaining the highly noisy signals. To overcome this difficulty, it is required to evaluate the signal to noise (S/N) ratio. In the present paper, the S/N ratio is defined by the ratio between the peak defect and no defect signals.

Fig. 13 shows results for the S/N ratios. As shown in Fig. 13, the S/N ratio is inversely proportional to the magnitude of liftoff. Comparison of the results in Figs. 12 and 13 suggests that our ∞ coil is superior S/N ratio to the others. Thus, we have succeeded in developing ∞ coil having a higher sensibility compared with those of conventional one.

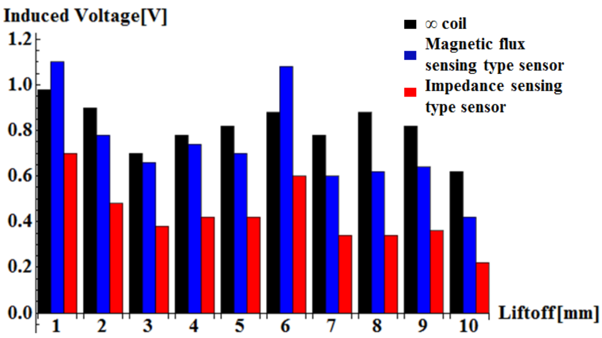

Fig. 12 Peak signal magnitude vs. liftoff

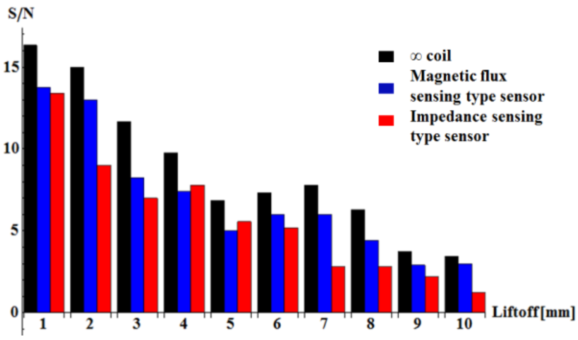

Fig. 13 S/N Ratio vs. liftoff

Conclusion

As shown above, we have succeeded in innovating and optimizing a new high sensibility eddy current sensor "∞ coil".

All of the 2D and 3D finite elements simulations were carried out by the finite element package "Femtet" produced by Murata Software Co. Ltd.

References

[1] I.Marinova, S.Hayano and Y.Saito, Ployphase eddy current testing, Journal of Applied Physics, Vol. 75, No.10, pp. 5904-5906, 1994.

[2] N.Burais and A.Nicolas, Electromagnetic field analysis in remote field eddy current testing systems, IEEE Transactions on Magnetics, Vol.25, No.4, pp.3010-3012, 1989.

[3] S.McFee and J.P.Webb, Automatic mesh generation for h-p adaption, IEEE Transactions on Magnetics, Vol.29, No.2, pp.1894-1897, 1993.

Enhance the Sensibility of the Eddy Current Testing

Kouki MARUYAMA[1, a], Illiana MARINOVA[2,b]
and
Yoshifuru SAITO[1,c]
[1] Graduate School of Hosei University, Tokyo 184-8584, Japan
[2] Technical University of Sofia, Sofia 1756, Bulgaria
[a] kouki.maruyama.8n@stu.hosei.ac.jp, [b] iliana@tu-sofia.bg, [c] ysaito@hosei.ac.jp

Keywords: ECT, resonance, sensibility.

Abstract. Eddy current testing (ECT) is one of the most representative nondestructive testing methods for metallic materials, parts, structures and so on. This paper proposes improvement of sensibility of the impedance sensing type ECT. Sensibility of the ECT is improved by means of three steps. One is an optimum exciting frequency selection. We employ the natural parallel resonant frequency of ECT coil. The second is to increase the sharpness of the resonance curve on impedance versus frequency characteristic by changing the coil connection. Finally, we attach externally capacitor to reduce the resonance frequency into low. This makes it possible to enhance the sensibility of the impedance sensing type ECT operating at the resonant frequency.

Introduction

Modern engineering products such as air-plane, automobile, smart building, high speed train and so on are essentially composed of metallic materials for forming the shape of product, suspending the mechanical stress and constructing the structural frames.

Among various nondestructive methods, ECT does not require complex electronic circuits and direct contact to target. Furthermore, target whose major frame parts are composed of conductive metallic materials can be selectively inspected by ECT.

Operating principle of the ECT is based on the two major properties of magnetic field. One is that exposing the conductive materials to the alternating magnetic fields induces eddy current in all of the conducting materials. Thereby, the input impedance of the magnetic field source, i.e., electric source, can detect the change of the target impedance caused by defects blocking eddy current flowing. The ECT based on this principle is called impedance sensing type. The other type utilizes a separately installed sensor coil to detect the leakage magnetic flux change. The magnetic field of ECT is composed of two components: one is the exciting and the other is the reactive component of magnetic fields. The reactive component of magnetic field is caused by the eddy currents in the target so that change of eddy current paths changes the reactive magnetic fields. Thus, the independently installed sensor detects this magnetic field change. This type is called a separately sensing coil type.

This paper proposes improvement of sensibility of the impedance sensing method. Improvement of the sensibility is carried out in the three major steps. The first is to select the optimum exciting frequency. We select the natural parallel resonant frequency of the ECT sensor coil when facing with a wholesome part of target. A system comprising the ECT facing with the wholesome part of target takes the maximum pure resistive impedance. When the ECT sensor coil meets with a defect of target, this resonance condition is essentially not satisfied. This makes it possible to maximize the difference between the resonance and not resonance impedances. The second step is to increase the resonant impedance as well as to sharpen the peaky impedance versus frequency characteristic by changing the coil connection. Since the natural parallel resonant impedance become larger, then the deviation between the resonant and not resonant impedances is essentially larger. This essentially enhances the sensibility of ECT sensor. Finally we attach an external capacitor to reduce the resonant frequency into low and also to enhance the sensibility.

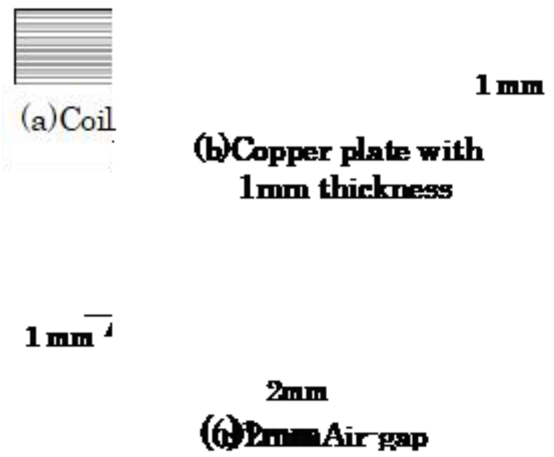

Fig.1 Tested coil and the measurement conditions.

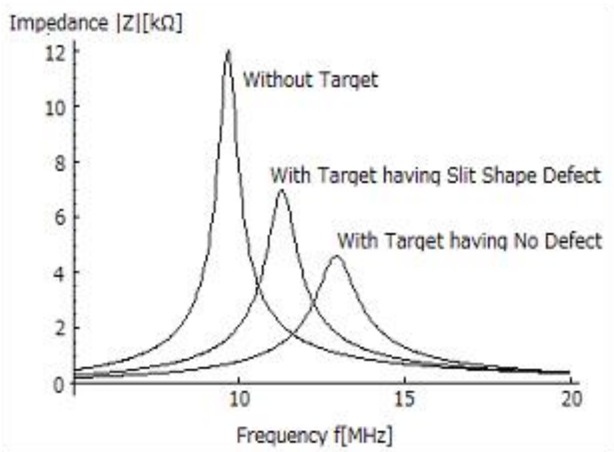

(a) Impedance |Z| vs. Frequency f.

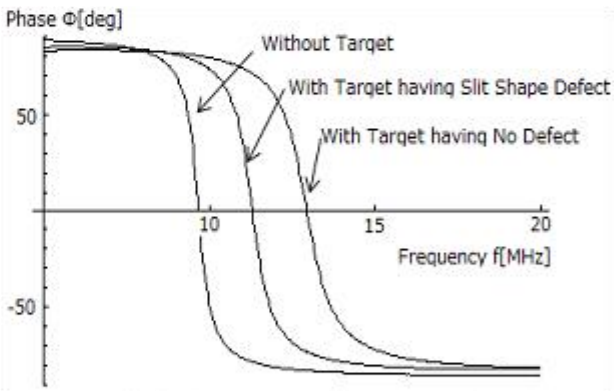

(b) Phase φ vs. Frequency f.

Fig.2 Frequency characteristics of the impedance and phase.

Operating principle of ECT. Let an arbitrary finite length solenoid coil shown in Fig. 1(a) be an eddy current sensor coil. When we put this sensor coil on a copper plate as shown in Fig. 1(b) and apply an alternating current to the sensor coil, because of the Faraday's law, eddy current is induced as a reaction of the alternating magnetic fields. Measure the input impedance of the sensor coil is able to diagnose a difference of the target copper plate condition between no defects (Fig. 1(b)) and 2mm crack defect (Fig. 1(c)). This is similar to the secondary impedance change detection from primary input terminal in a conventional single phase transformer. Thus, it is obvious that a simple finite length solenoid coil can detect the defects of the target conducting materials. This is the operating principle of impedance sensing type ECT.

Natural resonance phenomena of ECT coil. Any of the coils always exhibit an inductive property because of the magnetic fields around them by applying a current into the coil. However, any of the coils have the capacitances among the coils. Even though a simple finite length solenoid coil shown in Fig. 1(a), it is possible to observe its natural resonance phenomena as shown in Fig. 2. Figs 2(a) and 2(b) are the frequency f versus impedance |Z| and the frequency f versus phase ϕ characteristics, respectively.

Optimum operation frequency. Decision of ECT operation frequency is of paramount importance, because sensibility and searching depth of ECT are greatly depending on the operation frequency. Theoretically, the operation frequency of ECT can be decided by taking the target conductivity and its skin-depth into account. However, final selection of operation frequency is determined by the past experiences and the practical tests.

In the present paper, we select the natural parallel resonant frequency of the ECT sensor coil when facing with a wholesome part of target. The ECT facing with the wholesome part of target takes the maximum pure resistive impedance. When the ECT sensor coil meets with a defect of target, the resonance condition is essentially not established. Therefore, the input impedance from sensor coil input terminals is also reduced to small in value compared with those of the resonant one. Namely, a deviation between the resonance and not resonance impedances becomes maximum value.

A sensibility ε of ECT is defined by

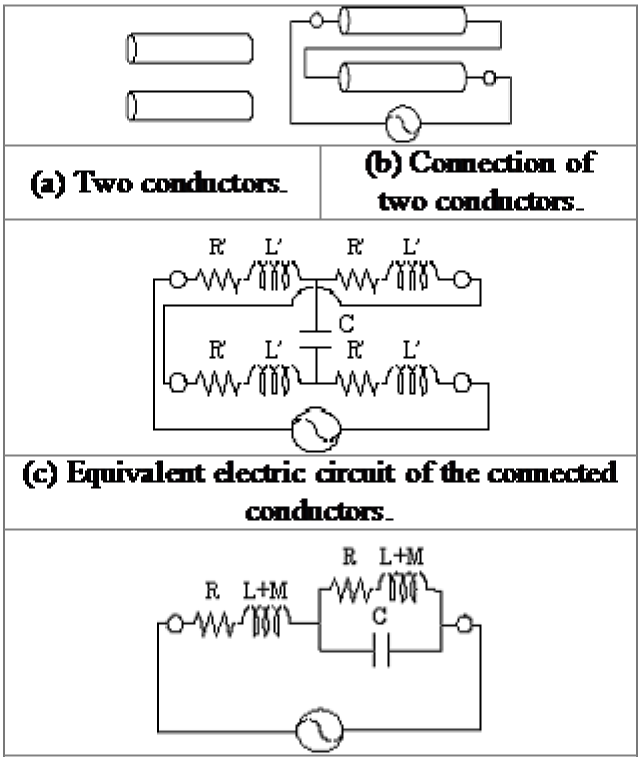

(a) Two conductors. (b) Connection of two conductors.

(c) Equivalent electric circuit of the connected conductors.

(d) Modified equivalent electric circuit of the connected conductors.

Fig.3 Principle of a resonance coil connection.

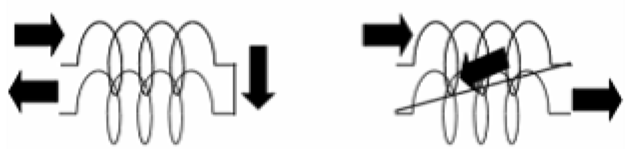

(a) Normal (b) Resonance type

Fig.4 Comparison of the normal with resonant coil connections.

Fig. 5 Example of a pair of twisted coils

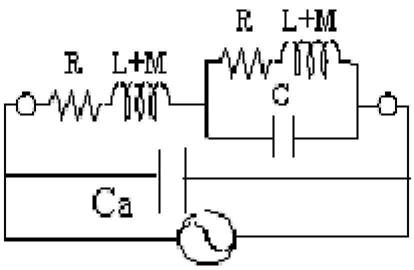

Fig.6 Externally attachment of capacitor Ca

$$\varepsilon = \frac{|reference - measured|}{reference} \times 100[\%] \quad , \quad (1)$$

where the reference and measured in (1) refer to the input impedances from the ECT coil terminals when facing the ECT coil with the wholesome and defect parts of target, respectively.

Enhancement of quality factor Q. The sensibility of (1) is intrinsically depended on the quality factor Q of the parallel resonance defined by

$$Q = \frac{f_0}{\Delta f} \quad , \quad (2)$$

where f_0 and Δf are the resonant frequency and the half width, respectively.

The quality factor Q represents a sharpness of the resonance curve on the impedance versus frequency coordinate. So that high Q in (2) means high sensibility in (1).

To increase the quality factor Q, we employ the resonant connection shown in Fig. 3. Figs. 3(a) and 3(b) are the two parallel conductors and their resonant connection, respectively.

Denoting R, L, M as the resistance, self-inductance and, mutual inductance, it is possible to draw an equivalent circuit of the resonant connected two conductors as shown in Figs. 3(c), 3(d). Fig.4 shows a difference between the normal and resonant coil connection [4].

Practically, the resonant connection is carried out by twisting the two coils to uniform the facing side of both conductors as shown in Fig. 5 [5].

Reduction of the resonant frequency. As mentioned above, the ECT operation frequency is of paramount importance, because sensibility and searching depth of ECT are greatly depending on the operation frequency. Therefore, we employ the natural parallel resonant frequency of ECT coil as operation frequency. But the resonantce frequency of ECT coil is relatively high. This means a low skin depth of the eddy currents in target. Thereby, searching depth is limited to only the vicinity of target surface. To overcome this problem, we attach externally capacitor C_a in parallel to the originally sensor coil circuits as shown in Fig.6. The resonant mode in Fig.2 is one of the parallel resonance phenomena so that attachment of capacitor C_a reduces the resonance frequency to low.

Experiment

Table 1. Various constants of the tested ECT coils.

	Conductor length	60cm
	Diameter of conductor	0.1mm
	Axis core	Ferrite bar (MnZn)
	Coil outer diameter	2.4mm
	Coil inner diameter	2mm
	Coil length	4mm
	Number of twisted turns	175/m
	Number of coil layers	3

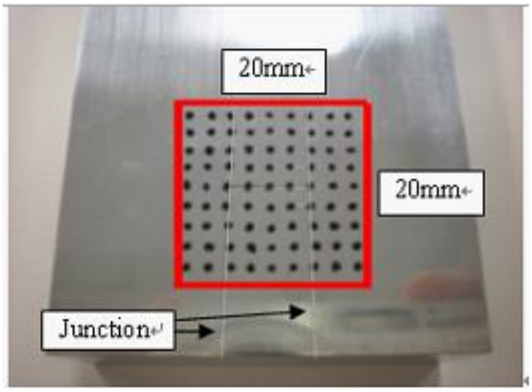

Fig. 7 Target test piece and measured points.

Fig. 8 Effect of the externaly attached capacitor C_a to the resonance impedances.

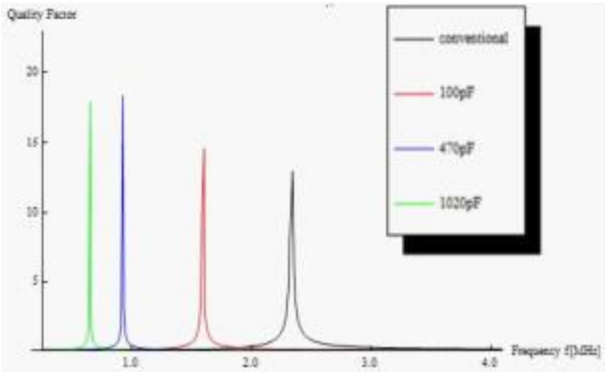

Fig.9 Improvement of quality factor Q

Tested target piece and tested ECT coils. Fig. 7 shows a target piece whose material is SUS304 steel. A vertical line shape artificial crack having 10mm length, 0.2mm width and 0.5mm depth had been made to the sandwiched SUS by the electrical discharge machining. Hereby, there is a junction of SUS at the both ends of the defect. In Fig. 7 a red square shows a 20mm by 20mm target area. The ECT sensors measured at the 9 by 9 sampling points with 2.5mm regular spacing on this 20mm by 20mm square area.

Table 1 lists the various constants of the tested ECT coils. The tested coil was wound around the Manganese-Zinc type ferrite bar used as an axial Ferrite core. Further, the coil was twisted 175/m to compose the resonant connection as described in Fig.3.

Reduction of the resonant frequency. We compare the resonance frequencies when attaching the external capacitors C_a and without external capacitor. Fig. 8 shows the effect of C_a to the resonant frequencies when facing on the target without any defects. Obviously, larger external capacitor C_a makes it possible to reduce the resonant frequency.

Eventhough, we have succeeded in reducing the resonant frequency into low, the resonant impedance becomes smaller inversely proportion to the magnitude of attached capacitance C_a. This may mean that the sensibility defined by (1) may be smaller in value when attaching a larger capaciatnce C_a.

To check this more specifically, we evaluated the quality factor Q defined by (2). Fig. 9 shows the quality factor Q when attaching the external capacitors C_a. According to the results in Fig. 9, it is found that an attachment of larger capacitance C_a improves the quality factor Q but too large capacitor C_a reduces the quality factor Q. This is because attachment of the very large capacitor C_a to the sensor circuit in parallel shown in Fig. 6 dominates an entire impedance, i.e., major current flows through the externally attached capacitor C_a but through not the sensor circuits.

Resonance type ECT operating at 256kHz. Since the 256kHz operation frequency is one of the most conventional operating frequencies on the current used ECTs, we have carried out the defect serchings employing the 256kHz operating frequency to check the effect of externallty attached capacitor C_a in parallel to the sensor coils.

Fig.10 shows the results of defect searching facing the target having the defect located at 0.1mm liftoff. Observe the results in Fig. 10 suggests that any of the results visualize the H character shape composed of the artificial defect and two mechanical junctions. In addition, the results in Fig. 10 suggest that the sensibilities are not depending on the attached externally capacitors C_a, i.e., any externally attached capacitors C_a in parallel to the sensor coils hardly change the original sensibility when operating 256kHz frequency.

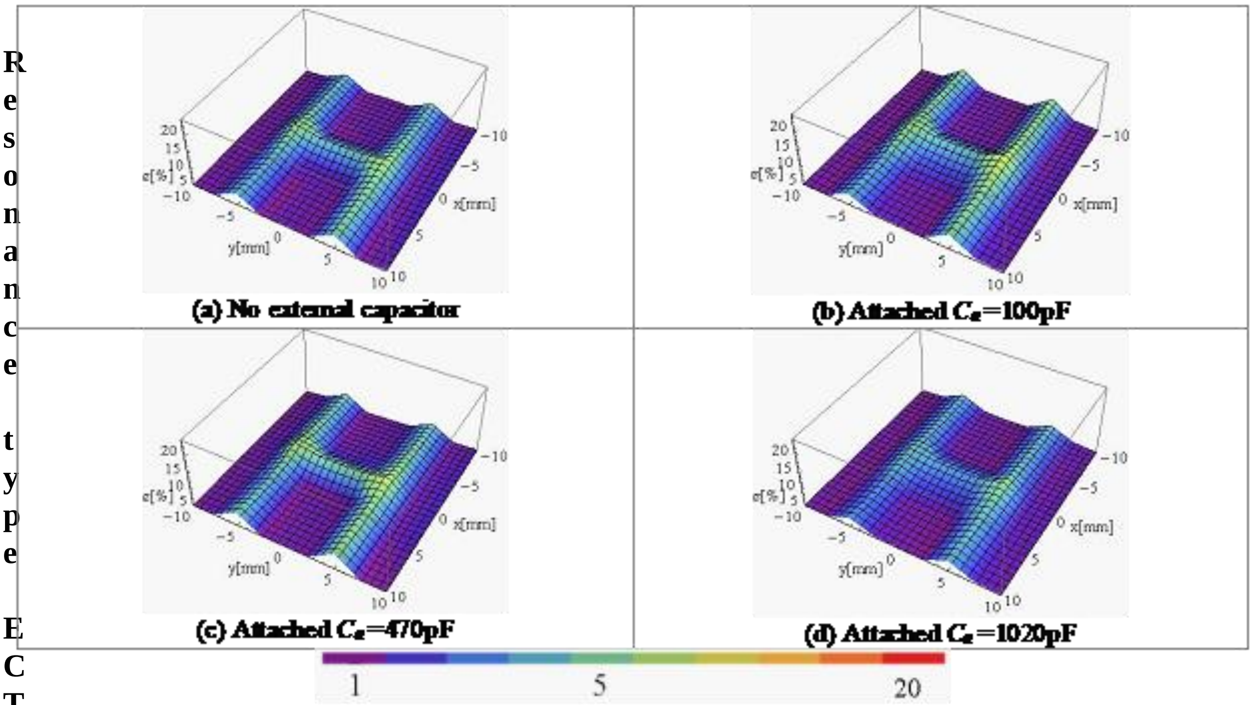

(a) No external capacitor (b) Attached C_a=100pF (c) Attached C_a=470pF (d) Attached C_a=1020pF

Fig. 10 Defect searching results operating with 256kHz frequency.

Resonance type ECT operating at the resonant frequency. When the tested ECT coil is facing to the target having the defect located at 0.1mm liftoff, attach externally capacitors C_a having the 0pF, 100pF, 470pF, 1020pF yields the resonant frequency 2350kHz, 1700kHz, 985kHz, 860kHz, respectively.

Fig. 11 shows each of the defect searching results employing their distinct natural resonant frequencies.

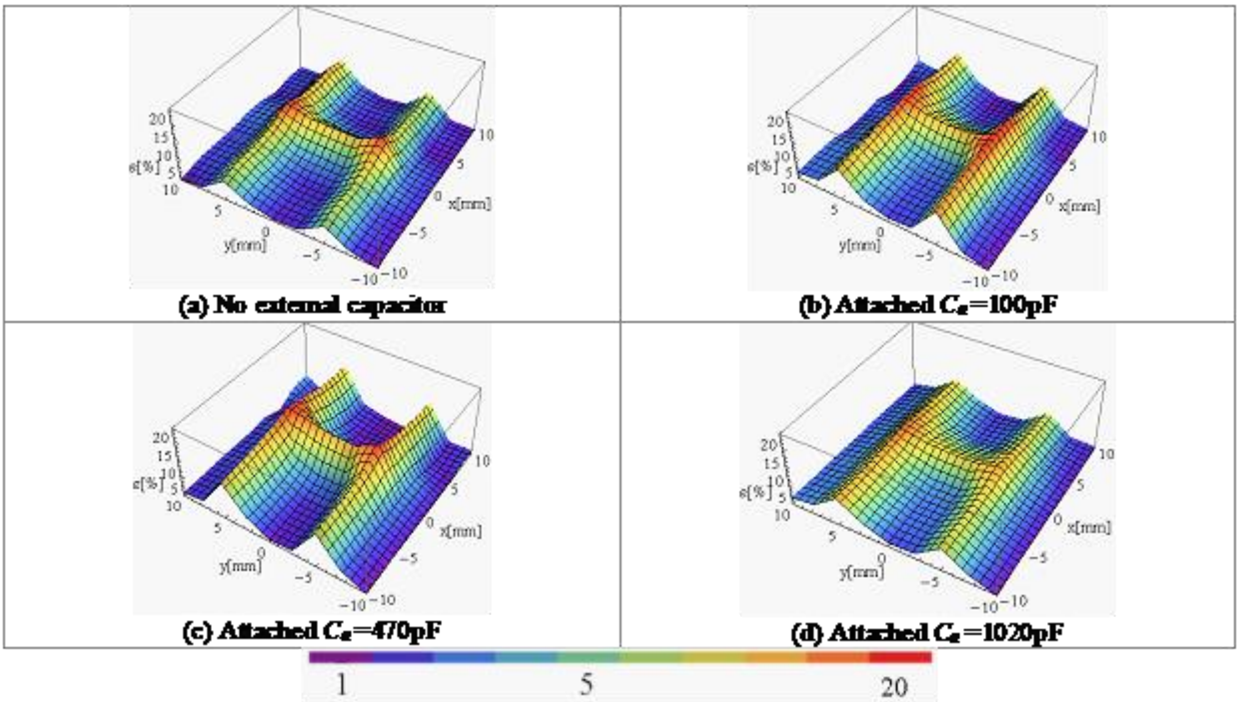

Fig. 11 Defect searching results operating with resonant frequency.

Comparison the quality factor Q in Fig. 9 and the detected results in Fig. 11 suggests that there is the optimum capacitance to reduced the resonant frequency, i.e. the C_a =470pF, to obtain the best detecting result. Also it has been confirmed that attachment of the very large capacitor C_a to the sensor circuit in parallel shown in Fig. 6 dominats an entire impedance, i.e., major current flows through the externally attached capacitor C_a but not the sensor circuits.

Conclusion

New innovative idea to enhance the sensibility of ECT sensor has been proposed in this paper. Our idea needs not any special tools but requires a consideration of natural resonance phenomena, i.e.utilization of the resonant impedance, frequency and capacitive effect among the coils and an externally attached capacitor.

We have selected the natural parallel resonant frequency of the ECT sensor coil when facing with a wholesome part of target. When the ECT sensor coil has met with a defect of target, the resonance condition has not been established. This led that the impedance reduced to small in value compared with those at resonance condition. As a result, a deviation between the resonant and not resonant impedances has become the maximum. Thus, the sensibility of ECT sensor has been enhanced.

Further, connection of the conductors to be applied a half of the source voltage to adjacent conductors has made it possible to enhance the capacitive effect among the conductors. Practically, this connection has been carried out by twisting the two coils to uniform the facing side of both conductors.

Finally, we have attached externally capacitors in parallel to the original ECT sensor coils. Attaching external capacitor has made it possible to increase the sensibility when a optimum external capacitance has been selected.

Thus, we have succeeded in working out one of the ultimate high sensibility resonance type ECT sensors.

References

[1] I.Marinova, S.Hayano and Y.Saito, Ployphase eddy current testing, Journal of Applied Physics, Vol. 75, No.10, pp.5904-5906, 1994.

[2] N.Burais and A.Nicolas,Electromagnetic field analysis in remote field eddy current testing systems,IEEE Transactionson Magnetics, Vol.25, No.4, pp.3010-3012, 1989.

[3] S. McFee and J. P. Webb, Automatic mesh generation for h-p adaption, IEEE Transactions on Magnetics, Vol. 29, No. 2, pp. 1894-1897, 1993.

[4] Y.Midorikawa, S.Hayano and Y.Saito, A resonant phenomenon between adjacent series connected coils and its application to a als, Advanced Computational and Design Techniques in Applied Electromagnetic Systems, Vol.6, pp. 633-639, 1995.

[5] S.Hayano, Y.Nakajima, H.Saotome and Y.Saito, A new type high frequency transformer, IEEE Transactions on Magnetics, Vol. 27, No.6, pp.5205-5207, 1991.